

# Transport driven by biharmonic forces: impact of correlated thermal noise

M. Machura<sup>1</sup> and J. Luczka<sup>1</sup>

<sup>1</sup>*Institute of Physics, University of Silesia, 40-007 Katowice, Poland*

We study an inertial Brownian particle moving in a symmetric periodic substrate, driven by a zero-mean biharmonic force and correlated thermal noise. The Brownian motion is described in terms of a Generalized Langevin Equation with an exponentially correlated Gaussian noise term, obeying the fluctuation-dissipation theorem. We analyse impact of non-zero correlation time of thermal noise on transport properties of the Brownian particle. We identify regimes where the increase of the correlation time intensifies long-time transport of the Brownian particle. The opposite effect is also found: longer correlation time reduces the stationary velocity of the particle. The correlation time induced multiple current reversal is detected. We reveal that thermal noise of non-zero correlation time can radically enhance long-time velocity of the Brownian particle in regimes where in the white noise limit the velocity is extremely small. All transport properties can be tested in the setup consisting of a resistively and capacitively shunted Josephson junction device.

PACS numbers: 05.60.-k, 05.40.-a, 85.25.Cp, 74.40.-n

## I. INTRODUCTION

Directed transport of particles can be driven by zero-average forces. The second principle of thermodynamics excludes it for systems at thermodynamic equilibrium. Therefore the system has to be at a nonequilibrium state and, moreover, some symmetries of the system have to be broken as e. g. the reflection symmetry of the spatially periodic potential or time-symmetry of the external force. Presence of both nonequilibrium conditions and asymmetry usually leads to transport and these two constituents form the ratchet concept. Transport in ratchet systems can be powered by mechanical, electrical, optical, chemical or electronic means. A large variety of models have been proposed and realized experimentally as solid state devices, cold atoms in optical lattices, superconducting devices, geometrically asymmetric lattices, to mention but a few, see the review [1].

The zero-average force can be deterministic or stochastic. An example of such a deterministic force is a time-periodic AC driving consisting of one or several harmonics. In some cases there is possibility of generating a charge or particle DC current from pure AC-driving, without the presence of an explicit static bias. The well-known phenomenon is harmonic mixing [2]. A paradigmatic model of this phenomenon is based on the Newton-Langevin equation which describes a particle moving in a spatially periodic potential (which mimics e.g. the motion of a charge particle in a crystal) and driven by biharmonic force  $F(t)$  of two components of frequencies  $\omega_1$  and  $\omega_2$  and amplitudes  $F_1$  and  $F_2$ , respectively,

$$F(t) = F_1 \sin(\omega_1 t) + F_2 \sin(\omega_2 t + \phi), \quad (1)$$

where  $\phi$  is the phase-lag of two signals. Transport in such systems has been studied in various contexts, mainly in the overdamped regime [3], for moderate damping [4], also in dissipative quantum systems [5], both experimentally and theoretically for cold atoms in the optical lattices [6–8], and for driven Josephson junctions [9].

The sketch of the paper is as follows. In Sec. II we briefly present main elements of modelling for typical systems exhibiting the ratchet effects when thermal fluctuations are described by Gaussian white noise. Sec. III contains the formulation of the corresponding model of non-Markovian dynamics for systems driven by biharmonic signals and correlated thermal noise. In Sec. IV we analyse in detail influence of correlation time of thermal noise on transport properties. Finally, Sec. V provides summary.

## II. PARADIGMATIC MODEL

An archetype of a ratchet is based on the Newton-Langevin equation

$$m\ddot{x} + \gamma\dot{x} = -V'(x) + G(t) + \xi(t), \quad (2)$$

where  $m$  is a mass of the particle,  $\gamma$  is the friction coefficient and  $V(x)$  is a spatially periodic potential of period  $L$ , i.e.  $V(x) = V(x + L)$ . The deterministic force  $G(t)$  is a non-biased function of zero average over some time-interval. The last term  $\xi(t)$  is a stochastic force which can model thermal equilibrium fluctuations and/or non-equilibrium noise.

Variations of this equation are unlimited. Putting formally  $m = 0$ , the overdamped system is modelled. In the case  $m \neq 0$ , inertial effects can be investigated. The potential  $V(x)$  can be symmetric or asymmetric, the force  $F(t)$  can be symmetric or not, the same for  $\xi(t)$  unless it mimics thermal noise, which is always symmetric. Problem of symmetry of the stochastic driving  $\xi(t)$  is discussed in Ref. [10].

If the process  $\xi(t)$  describes thermal equilibrium fluctuations then  $\xi(t)$  is zero-mean, Gaussian white noise with the Dirac delta auto-correlation function

$$\langle \xi(t)\xi(s) \rangle = 2\gamma k_B T_0 \delta(t - s), \quad (3)$$

where  $k_B$  the Boltzmann constant and  $T_0$  denotes the temperature. Note that this process is not correlated

and in consequence its correlation time  $\tau_c = 0$ . The noise intensity factor  $2\gamma k_B T_0$  follows from the fluctuation-dissipation theorem [11]. Gaussian white noise generates mathematically tractable models. In many real systems thermal noise is approximately white, meaning that the power spectral density is nearly equal throughout the frequency spectrum. Additionally, the amplitude of the signal has very nearly a Gaussian probability density function. However, an infinite-bandwidth white noise signal is purely a theoretical construction. By having power at all frequencies, the total power of such a signal is infinite and therefore impossible to generate. In practice, however, a signal can be "white" with a flat spectrum over a defined frequency band and it is a good approximation of many real-world situations. E.g. in electrical systems, the white noise modelling is correct at any practical radio frequency in use (i.e. frequencies below about 80 GHz). In the most general case, which includes up to optical frequencies, the power spectral density of the voltage across the resistor depends on frequency and the white noise approximation fails.

In the paper, we study transport in a spatially symmetric substrate and the corresponding potential is reflection symmetric, i.e.  $V(x_0 + x) = V(x_0 - x)$  for some fixed value  $x_0$ . One of the simplest form of such a potential is given by the sinusoidal form

$$V(x) = \Delta V \sin(2\pi x/L) \quad (4)$$

of the period  $L$  and the barrier height  $2\Delta V$ . The non-equilibrium driving  $G(t)$  is a biharmonic force and is chosen as a particular case of Eq. (1), namely,

$$G(t) = A[\sin(\Omega t) + \varepsilon \sin(2\Omega t + \phi)]. \quad (5)$$

Here  $A$  is the amplitude of the first harmonic, the factor  $\varepsilon$  scales the second harmonics, so that it has the resulting amplitude  $\varepsilon A$ . The angular frequency  $\Omega$  determines the time period  $T = 2\pi/\Omega$  of the driving and  $\phi$  controls the phase shift between two components of the biharmonic signal (5), see Fig. 1 for details.

The Langevin equation (2) with the potential (4) has a similar form as an equation describing dynamics of the phase difference  $\Psi = \Psi(t)$  between the macroscopic wave functions of the Cooper pairs on both sides of the resistively and capacitively shunted Josephson junction, which is well known in the literature as the Stewart-McCumber model [12, 13], namely,

$$\begin{aligned} \left(\frac{\hbar}{2e}\right)^2 C \ddot{\Psi} + \left(\frac{\hbar}{2e}\right)^2 \frac{1}{R} \dot{\Psi} + \frac{\hbar}{2e} I_0 \sin \Psi \\ = \frac{\hbar}{2e} I(t) + \frac{\hbar}{2e} \sqrt{\frac{2k_B T}{R}} \xi(t). \end{aligned} \quad (6)$$

The left hand side is the total current through the junction. It is a sum of three additive current contributions: a displacement current accompanied with a capacitance  $C$  of the junction, a normal (Ohmic) current characterized by the normal state resistance  $R$  and a Cooper pair tunnel supercurrent characterized by the critical current  $I_0$ .

In the right hand side,  $I(t)$  is an external current. The Johnson noise  $\xi(t)$  plays a role of thermal equilibrium noise associated with the resistance  $R$  and is modelled by Gaussian white noise of zero mean and the intensity taken according to the fluctuation-dissipation theorem. It is an evident correspondence between two models: the coordinate  $x = \Psi - \pi/2$ , the mass  $m = (\hbar/2e)^2 C$ , the friction coefficient  $\gamma = (\hbar/2e)^2 (1/R)$ , the barrier height is determined by the relation  $\Delta V = (\hbar/2e) I_0$  and the period  $L = 2\pi$ . The biharmonic signal  $G(t)$  in Eq. (5) corresponds to the external current  $I(t)$ . The velocity  $v = \dot{x}$  corresponds to the voltage  $V$  across the junction. This correspondence allows for testing all transport properties of the system (2) and its generalizations by the setup consisting of a resistively and capacitively shunted Josephson junction device.

### III. NON-MARKOVIAN DYNAMICS

If the correlation time  $\tau_c$  of thermal noise is much smaller than the smallest characteristic (deterministic) time  $\tau_x$  in the considered system then the white noise modelling is a good approximation. However, there are systems where this relation is not satisfied: the noise correlation time can be of order or greater than  $\tau_x$  [14–16]. In this case we shall not assume the Markovian dynamics but rather invoke the Generalized Langevin Equation (GLE) for the time evolution of the system (2).

When the correlations comes into play the dynamics becomes non-Markovian and exhibits the memory-friction described by the GLE in the form [11, 15, 17, 18]

$$m\ddot{x}(t) + \int_0^t K(t-s)\dot{x}(s) ds = -U'(x(t), t) + \xi(t), \quad (7)$$

where  $\xi(t)$  is a stationary, zero-mean Gaussian stochastic process modelling correlated thermal noise and the full potential takes the form

$$U(x, t) = V(x) - A[\sin(\Omega t) + \varepsilon \sin(2\Omega t + \phi)]x. \quad (8)$$

The auto-correlation function  $C(t-s)$  of the correlated Gaussian thermal noise  $\xi(t)$  is related to the memory kernel  $K(t)$  via the fluctuation-dissipation relation [11, 15, 17, 18]:

$$C(t-s) = \langle \xi(t)\xi(s) \rangle = k_B T_0 K(|t-s|). \quad (9)$$

Let us note that for more realistic modelling based on correlated thermal fluctuations we have to pay the price: Eq. (7) is an integro-differential equation with a Gaussian random term which is difficult to handle by analytical or numerical means. The resulting process is neither Gaussian nor Markovian. In a general case, we do not know even a master equation for the single-event non-Markovian probability  $p(x, \dot{x}, t)$  of the process determined by Eq. (7). However, the problem is much easier to treat if the non-Markovian process  $x(t)$  is a projection of a higher-dimensional Markovian process. In other

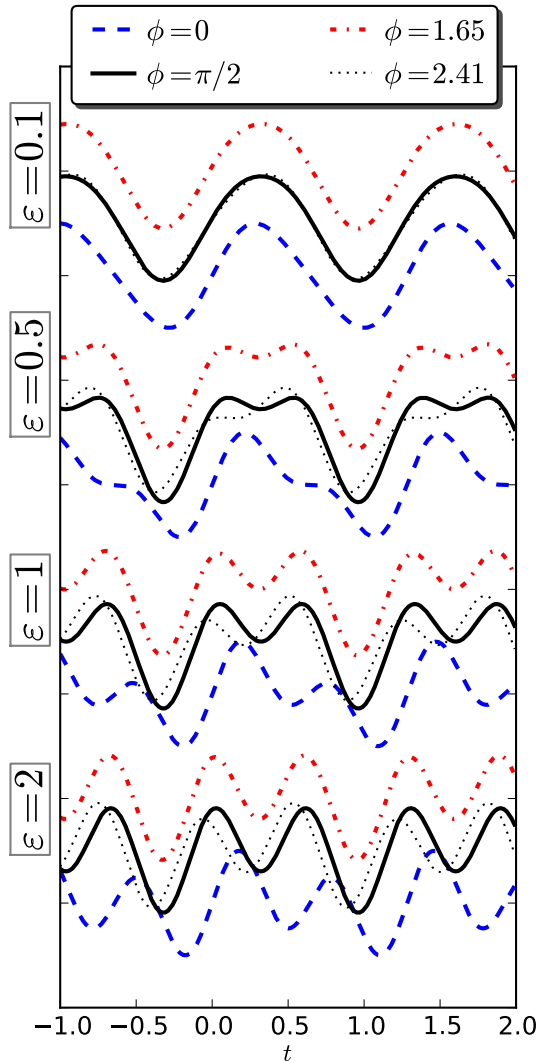


FIG. 1: (color online) Biharmonic external ac driving  $G(t) = A[\sin(\Omega t) + \varepsilon \sin(2\Omega t + \phi)]$  plotted for amplitude  $A = 1$  and frequency  $\Omega = 1$ , for four different second harmonic amplitude  $\varepsilon = 0.1, 0.5, 1, 2$  and four phase shifts  $\phi = 0, \pi/2, 1.65, 2.41$  which corresponds to the later commented figures (see 3 and 4 for details).

words, it can be embedded in a higher (but finite) dimensional phase space and then Eq. (7) can be converted to a set of first-order differential equations of Langevin type. It can be done if the kernel  $K(t)$  obeys an ordinary differential equation with constant coefficients.

### A. Correlated thermal noise

Gaussian thermal noise  $\xi(t)$  is completely defined by its correlation function  $C(t)$ . White noise corresponds to

(3). Examples of correlated noise are: the exponentially correlated noise [19], harmonic noise [20], algebraically correlated noise [21, 22]. Other variations of noise are also considered, as e.g. when  $C(t)$  is a sum of exponentials [22–24].

The simplest correlated noise is exponentially correlated noise (because of the smallest number of parameters) known as the Ornstein-Uhlenbeck (O-U) stationary stochastic Markov process for  $\xi(t)$  [15]. Its correlation function reads

$$\langle \xi(t)\xi(s) \rangle = k_B T_0 K(|t-s|) = \frac{\gamma k_B T_0}{\tau_c} e^{-|t-s|/\tau_c}. \quad (10)$$

Here  $\tau_c$  is the correlation time of the O-U process. When the correlation time  $\tau_c \rightarrow 0$  the correlation function (10) tends to the correlation function (3) and the O-U process tends to white noise. Then Eq. (7) reduces to Eq. (2). Below, we study the case of O-U noise.

### B. Markovian embedding dynamics

For the case of the O-U noise, the integral kernel (9) is an exponential function of the time. The exponential function obeys a first-order differential equation with a constant coefficient. Therefore we can convert the integro-differential equation (7) into a set of ordinary stochastic differential equations. To this aim we define the auxiliary stochastic process

$$w(t) = \frac{\gamma}{\tau_c} \int_0^t e^{-(t-s)/\tau_c} \dot{x}(s) ds, \quad (11)$$

which is an integral part of Eq. (7). By means of the above relation the GLE (7) can be rewritten in the form

$$m\dot{v}(t) = -U'(x(t), t) - w(t) + \xi(t), \quad (12)$$

$$\dot{x}(t) = v(t), \quad (13)$$

$$\dot{w}(t) = -\frac{1}{\tau_c} w(t) + \frac{\gamma}{\tau_c} v(t), \quad (14)$$

$$\dot{\xi}(t) = -\frac{1}{\tau_c} \xi(t) + \frac{1}{\tau_c} \sqrt{2\gamma k_B T_0} \Gamma(t), \quad (15)$$

The last equation (15) corresponds to the O-U process with the exponential correlation function in Eq. (10) [25]. The stationary stochastic process  $\Gamma(t)$  describes Gaussian white noise of zero mean and correlation function  $\langle \Gamma(t)\Gamma(s) \rangle = \delta(t-s)$ . So, we embedded a non-Markovian process in a 4-dimensional space in which the process is Markovian. It is not a minimal dimension. It can be further reduced to the 3-dimensional space. To do it, let us note that for the linear combination  $z(t) = \xi(t) - w(t)$  we are able to subtract the two last relations and reproduce the three coupled Langevin equations [26], namely,

$$\dot{x}(t) = v(t), \quad (16)$$

$$\dot{v}(t) = -\frac{1}{m} U'(x(t), t) + \frac{1}{m} z(t), \quad (17)$$

$$\dot{z}(t) = -\frac{1}{\tau_c} z(t) - \frac{\gamma}{\tau_c} v(t) + \frac{1}{\tau_c} \sqrt{2\gamma k_B T_0} \Gamma(t). \quad (18)$$

In the following we shall analyse this set of three coupled equations.

### C. Dimensionless variables

The natural length scale for the system is settled by the period  $L$  of the potential  $V(x)$ . For the adequate time scale we have to consider several time scales [27]. Here we define the characteristic time as  $\tau_0^2 = mL^2/\Delta V$  which is convenient for studying inertial effects. It can be obtained from Eq. (2) by comparing the inertial term (with mass  $m$ ) to the potential force  $V'(x)$  and inserting in both sides the characteristic quantities, for detail see Ref. [27]. It leads to the scaling used throughout this paper

$$X = \frac{x}{L}, \quad \hat{t} = \frac{t}{\tau_0}, \quad (19)$$

and finally to the rescaled evolution equations

$$\dot{X} = Y, \quad (20)$$

$$\dot{Y} = -W'(X) + a[\sin(\omega\hat{t}) + \varepsilon \sin(2\omega\hat{t} + \phi)] + Z, \quad (21)$$

$$\dot{Z} = -\frac{1}{\hat{\tau}_c}Z - \frac{\hat{\gamma}}{\hat{\tau}_c}Y + \frac{1}{\hat{\tau}_c}\sqrt{2\hat{\gamma}D}\hat{\xi}(\hat{t}), \quad (22)$$

where the explicit form of remaining coordinates reads

$$Y = \frac{\tau_0}{L}v, \quad Z = \frac{L}{\Delta V}z. \quad (23)$$

The dot and prime denote the differentiation with respect to the scaled time  $\hat{t}$  and the argument respectively. Rescaled velocity is designated by  $Y(\hat{t})$  and  $Z(\hat{t})$  symbolizes the dimensionless random force. The remaining re-scaled parameters are:

1. the friction coefficient  $\hat{\gamma} = (\gamma/m)\tau_0 = \tau_0/\tau_L$  is defined by the ratio the two characteristic times of the GLE - previously defined  $\tau_0$  and the relaxation time of the velocity degree of freedom  $\tau_L = m/\gamma$ ,
2. the correlation time  $\hat{\tau}_c = \tau_c/\tau_0$ ,
3. the potential  $W(X) = V(x)/\Delta V = W(X+1) = \sin(2\pi X)$  possesses the unit period and barrier height  $\Delta\hat{V} = 2$ ,
4. the amplitudes of the external deterministic stimulus scales as  $a = LA/\Delta V$  and the frequency  $\omega = \Omega\tau_0$  (or the equivalent period  $T = 2\pi/\omega$ ),
5. the zero-mean white noise  $\hat{\xi}(\hat{t})$  is correlated as  $\langle\hat{\xi}(\hat{t})\hat{\xi}(\hat{s})\rangle = \delta(\hat{t}-\hat{s})$  with a re-scaled noise intensity  $D = k_B T_0/\Delta V$  and can be interpreted as the ratio of two energies, thermal energy and half of barrier height of the potential  $V(x)$ .

From now on we will use only above dimensionless variables and shall omit the ‘‘hats’’ in all quantities of Eqs. (20)-(22).

### D. Method of analysis

The analytical methods to handle nonlinear Brownian equations with memory friction are unknown to our knowledge. Therefore we will explore the peculiarities of the system (20)-(22) by means of numerically calculated long-time transport characteristics. In particular we shall focus on the current defined by the long-time averaged velocity  $v \equiv \langle Y \rangle$ . The averaging is performed in the following way: First the numerical mean over at least  $10^3$  realizations of the GLE is calculated. This yields a time dependent quantity which we next average over one period of the external field  $T$ . In the process of calculating averages we must make sure that we initiate the process evolutions with unbiased initial conditions since the simulated asymptotic, long time dynamics is not necessarily ergodic. We choose all initial positions and velocities to be uniformly distributed over one potential period  $[0, 1]$  and the interval  $v \in [-2, 2]$ , respectively. From the technical point of view we have employed Stochastic Runge-Kutta algorithm of the 2<sup>nd</sup> order [28] with the time step of  $[10^{-3} \div 10^{-4}]T$ . All numerical calculations have been performed using CUDA environment on desktop computing processor NVIDIA Tesla C1060 [29].

### IV. IMPACT OF CORRELATED THERMAL NOISE ON TRANSPORT

In the long time limit, the averaged velocity can be presented in the form of a series of all possible harmonics, namely,

$$\lim_{t \rightarrow \infty} \langle \dot{X} \rangle = v + v_\omega(t) + v_{2\omega}(t) + \dots, \quad (24)$$

where  $v$  is a dc (time-independent) component and  $v_{n\omega}(t)$  are time-periodic functions which time average over a basic period are zero. In figures we present only the dc component  $v$  of the long time, averaged velocity. From the symmetry property of Eq. (7) it follows when  $v$  vanishes, for details see [8, 30–33]. In particular, in Ref. [31] it has been shown that if the force  $F(t)$  in Eq. (1) has the form

$$F(t) = \epsilon_1 \cos(q\omega t + \phi_1) + \epsilon_2 \cos(p\omega t + \phi_2) \quad (25)$$

and  $(p, q)$  are two coprime integers such that  $p + q$  is odd, the asymptotic velocity can be approximated by the expression

$$v = B\epsilon_1^p \epsilon_2^q \cos(p\phi_1 - q\phi_1 + \theta_0) \quad (26)$$

provided the amplitudes  $\epsilon_1$  and  $\epsilon_2$  are sufficiently small. The quantities  $B$  and  $\theta_0$  depend on the parameters of the model and  $\omega$  but neither on the amplitudes nor on the phases.

We remind that in the Hamiltonian regime Eq. (7) reduces to the form

$$m\ddot{x}(t) = -U'(x(t), t) \quad (27)$$

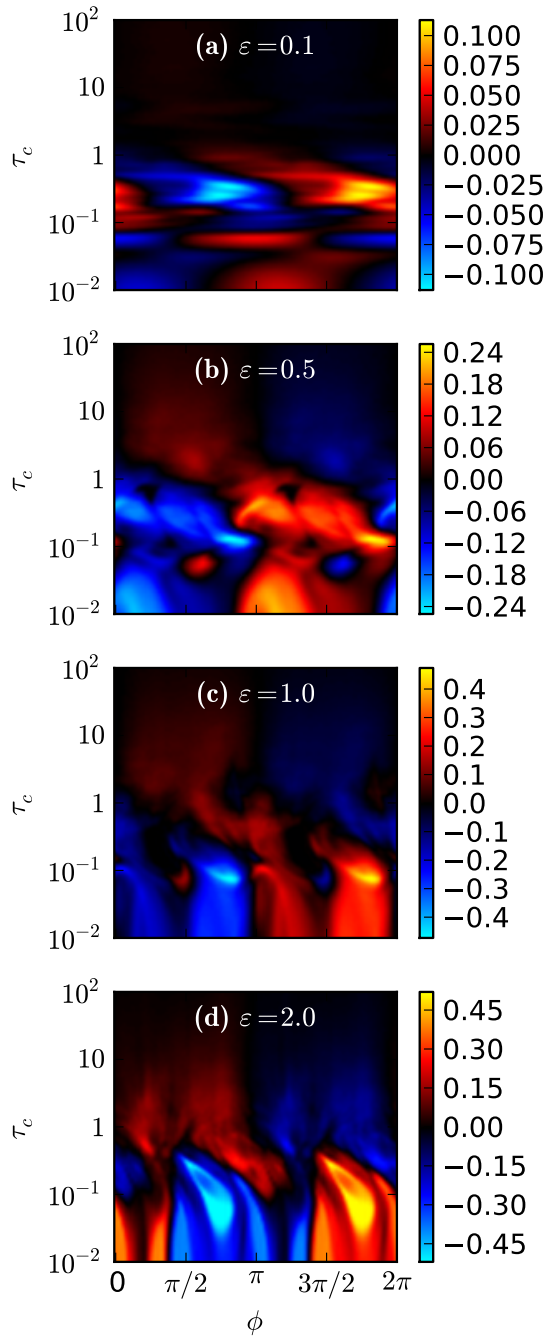


FIG. 2: (color online) Influence of the second harmonic of the external force  $G(t)$  on transport properties of the system (7) is presented. Dependence of the drift velocity on both the relative phase  $\phi$  (horizontal axis) and the correlation time  $\tau_c$  of thermal fluctuations (vertical axis) is depicted for increasing values of the amplitude  $\varepsilon$  of the biharmonic driving  $G(t)$  (top to bottom). The other rescaled parameters read  $a = 4.2$ ,  $\omega = 4.9$ ,  $\gamma = 0.9$ ,  $d_0 = 0.001$ .

and for small amplitudes the dc velocity takes the sine-like form [4, 34]

$$v \propto \sin \phi. \quad (28)$$

Mechanism of the transport generation in Hamiltonian systems is explained in Ref. [35]. The Hamiltonian regime can be realized in two case: (i) in the dissipationless regime when  $\gamma = 0$  and  $D = 0$ , (ii) in the limit of long correlation time,  $\tau_c \gg 1$ .

For white noise case and in the weak damping regime, the dissipation-induced phase lag  $\phi_0$  occurs, i.e. [4, 34]

$$v \propto \sin(\phi - \phi_0), \quad (29)$$

where the phase lag  $\phi_0$  is determined by dissipation and vanishes in the Hamiltonian limit.

We first address the issue of whether, and to which extent, the non-zero correlation time  $\tau_c$  of thermal fluctuations can influence transport properties. We thus start our analysis by studying the asymptotic dc velocity  $v$  as a function of both the time-symmetry breaking phase  $\phi$  and the correlation time  $\tau_c$ . Our results are shown in Fig. 2 for selected values of the driving amplitude  $\varepsilon$  of the second harmonics. A general conclusion from all cases presented in this figure is the destructive influence of the strongly correlated noise: for long correlation time  $\tau_c$  the dc velocity is much smaller (virtually zero) than for the small-to-moderate correlation time. Let us note that the limit of the long correlation time ( $\tau_c \gg 1$ ), corresponds to the Hamiltonian regime in which transport is non-effective in comparison with the dissipative regime. A more accurate inspection reveals regions of weakly correlated noise where reach diversity of transport characteristics can be observed. To identify them we search the section  $\phi = \text{const.}$  of a constant phase in Fig. 2. The results are depicted in Fig. 3 where the average velocity is plotted as a function of the correlation time for three selected values of the amplitude  $\varepsilon = 0.1, 1, 2$  (the same as in panels a, c and d of Fig. 2). The phase is fixed at the values  $\phi = 1.65$  and  $\phi = 2.41$ . In Fig. 3, one can identify the so termed current reversal phenomenon: the velocity changes its sign as one of the parameters is varied. Here, even the multiple current reversal can be observed by changing the noise correlation time. E.g. for the amplitudes  $\varepsilon = 1$  in Fig. 3(a), the average velocity is negative for white noise, i.e. when  $\tau_c = 0$ . If the correlation time  $\tau_c$  increases, the velocity approaches zero value: the particle does not exhibit directed transport. Upon further increasing of  $\tau_c$ , the velocity starts to increase to a positive-valued local maximum. Next, it again starts to decrease reaching a negative-valued local minimum. For further increase of  $\tau_c$ , the velocity tends again to a positive-valued local maximum. Finally, with increasing  $\tau_c$  it monotonically decreases towards smaller and smaller positive values.

As the next point of analysis, we ask about the positive role of weakly correlated noise, i. e. whether small  $\tau_c$  can intensify transport by enhancing the absolute value of

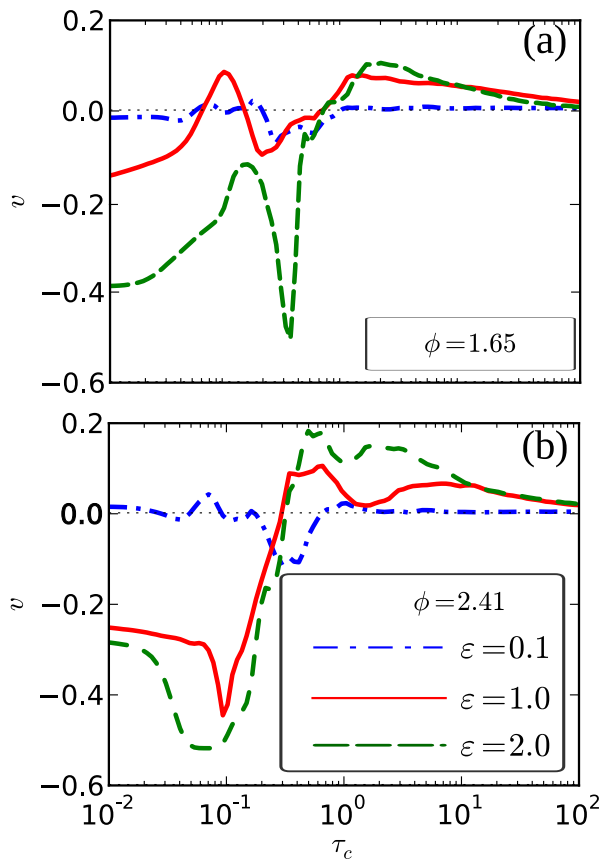


FIG. 3: (color online) The stationary averaged velocity  $v$  vs the correlation time  $\tau_c$  of thermal noise for three values of the relative amplitude  $\varepsilon$  of the second harmonics and two values of the relative phase  $\phi$ . Other parameters are:  $a = 4.2$ ,  $\omega = 4.9$ ,  $\gamma = 0.9$ ,  $d_0 = 0.001$ .

the average velocity. The answer is yes. As an example, consider the case  $\varepsilon = 2$  in Fig. 3(b). For  $\tau_c = 0$ , the velocity is negative and its absolute value is relatively large. If  $\tau_c$  starts to increase, the absolute value of the velocity also increases attaining a global maximum at some fixed value of  $\tau_c$  (of order  $10^{-1}$ ). In this example, the weakly correlated noise enhances transport in some interval of  $\tau_c$ . On contrary, for the same amplitude  $\varepsilon = 2$  but different value of the phase  $\phi = 1.65$ , if  $\tau_c$  starts to increase from zero, the absolute value of the velocity decreases, see the case  $\varepsilon = 2$  in Fig. 3(a).

The influence of temperature is depicted in Fig. 4, where two various regimes are illustrated. In panel (a) we show the same curve as in panel (a) of Fig. 3 (the case  $\varepsilon = 1$  and  $d_0 = 0.001$ ). In this regime we can note the most pronounced influence of temperature in vicinity of the first maximum: if temperature increases, the first maximum is significantly reduced and velocity even changes its sign. So, by changing the temperature one can obtain the current reversal, see the curves for  $d_0 = 0.001$  and  $d_0 = 0.01$  in panel (a). We have searched a wide part of the parameter space in order to locate re-

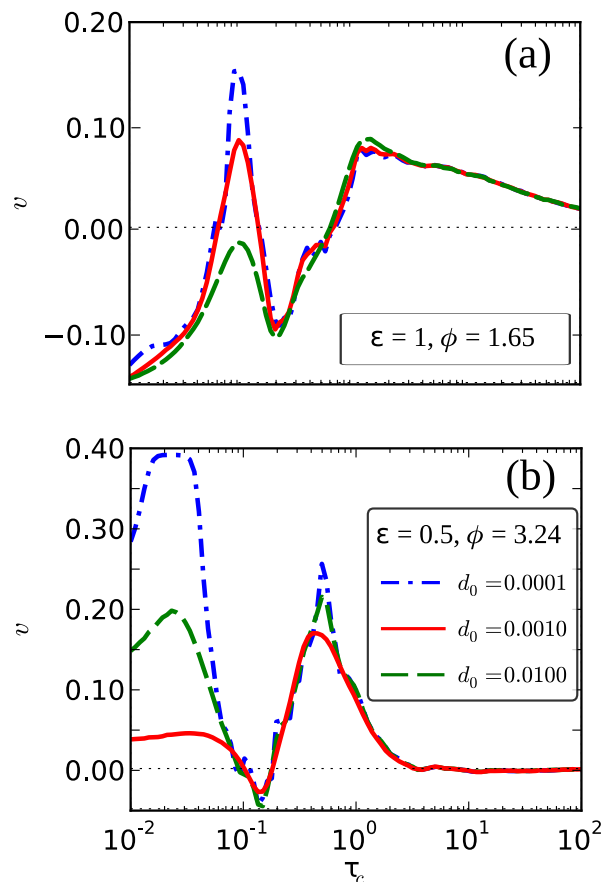


FIG. 4: (color online) The stationary averaged velocity  $v$  vs the correlation time  $\tau_c$  of thermal noise for three values of the relative temperature  $d_0 = 0.0001, 0.001, 0.01$  and two sets of pairs  $\varepsilon = 1, \phi = 1.65$  (panel a) and  $\varepsilon = 0.5, \phi = 3.24$  (panel b). Please note the destructive role of the small correlation time  $\tau_c$  on panel (a) and the antagonistic effect of the constructive impact of  $\tau_c$  in panel (b). For large values of  $\tau_c$  the average velocity is always much smaller and virtually is zero. Other parameters are:  $a = 4.2$ ,  $\varepsilon = 1$ ,  $\omega = 4.9$ ,  $\gamma = 0.9$ .

gions of temperature robustness. The conclusion is that for large values of the correlation time (in most cases  $\tau_c > 1$ ) the system is resistant to increase of temperature, at least to values presented in Fig. 4. On the contrary, for small correlation times, there are regimes where the system is sensitive to changes of temperature and increase of temperature responses in smaller values of the absolute value of velocity, see panel (b) of Fig. 4. It is a region of destructive role of temperature but the constructive role of short correlation times of thermal fluctuations: a first increase of  $\tau_c$  from zero results in increase of the velocity. For moderate and long correlation time, the temperature smooths the dependence on the correlation time similarly as in both panels of Fig. 4.

Finally, in Fig. 5 we present a regime where the amplitude of the second harmonics is much greater than the first harmonics (here 10 times greater). In such a case, the degree of symmetry breaking is very small: the in-



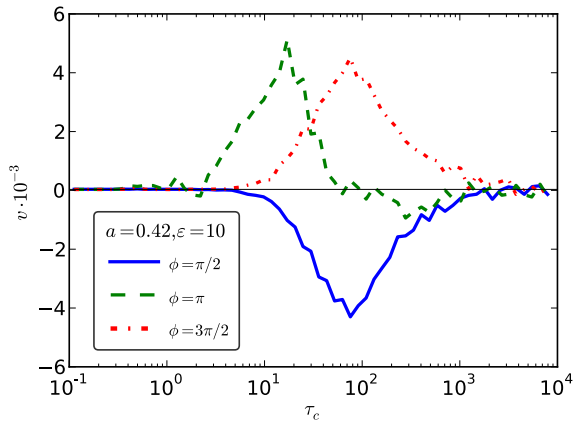


FIG. 5: (color online) The stationary averaged velocity vs the correlation time  $\tau_c$  of thermal noise for three values of the relative phase  $\phi = \pi/2$  blue (solid) line,  $\pi$  green (dashed) line,  $3\pi/2$  red (dashed-dotted) line. Other parameters are:  $a = 0.4$ ,  $\varepsilon = 10$ ,  $\omega = 4.9$ ,  $\gamma = 0.9$ ,  $d_0 = 0.001$ .

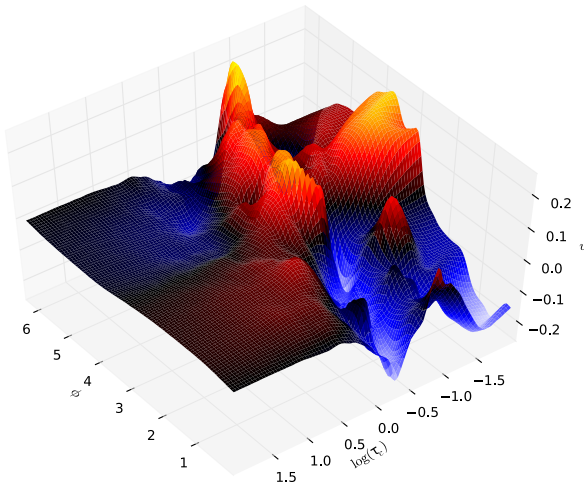


FIG. 6: (color online) Illustration of role of the thermal noise correlations and the relative phase of driving two harmonics on transport of the Brownian particle. It is a regime where long correlations of thermal noise destruct transport. The parameters:  $a = 4.2$ ,  $\varepsilon = 0.5$ ,  $\omega = 4.9$ ,  $\gamma = 0.9$ ,  $d_0 = 0.001$

fluence of the first harmonics is much smaller than the

second one (remember that if any of two harmonics is absent, there is no transport in the system). Therefore the dc velocity is expected to be extremely small (practically, it is zero). It is true but only for short correlation times (from 0 to 1 in Fig. 5). When we, however, increase  $\tau_c$  a little bit more and pass the value of about 1, the significant net transport occurs. For some values of the phase  $\phi$  the velocity is negative velocity ( $\phi = \pi/2$ ); for other values of  $\phi$  it shows the positive response ( $\phi = 3\pi/2$ ). In some other cases it exhibits the velocity reversal phenomenon as e.g. for  $\phi = \pi$ .

We have mainly concentrated the analysis on impact of the correlation time of thermal noise on transport properties of the Brownian particle. Other parameters modify directed movement as well. We do not present all varieties but yet we refer to our webpage [36] where the more detailed analysis is presented.

## V. SUMMARY

The richness and diversity of influence of non-zero correlation time of thermal noise on non-Markovian dynamics determined by Eq. (7) is summarized and visualized in Fig. 6. This picture looks like a landscape after intensive eruption of volcanoes: there are mountains with sharp summits and volcanoes with deep craters. This landscape can continuously be deformed to other complicated landscapes by changing parameters of the model. If you are long-suffering, you can discover your own original landscapes of non-Markovian dynamics driven by biharmonic signals. The diversity of subtle structures hidden in Eq. (7) is infinitely large. It comes to our mind a loose analogy to a Mandelbrot set which conceals beautiful forms of Julia sets, fractals and extremely difficult mathematics.

## Acknowledgments

The authors thank M. Januszewski for preparing the precise program (<http://gitorious.org/sdepy>) that we have used for numerical calculations. The work supported by the ESF Program "Exploring the Physics of Small Devices".

- [1] P. Hänggi and F. Marchesoni, *Rev. Mod. Phys.* **81**, 387 (2009).
- [2] C. E. Skov and E. Pearlstein, *Rev. Sci. Instr.* **35**, 962 (1964); W. Schnerder and K. Seeger, *Appl. Phys. Lett.* **8**, 133 (1966).
- [3] F. Marchesoni, *Phys. Lett. A* **119**, 221 (1986); M. Borromeo and F. Marchesoni, *Europhys. Lett.* **72**, 362 (2005); M. Borromeo, P. Hänggi and F. Marchesoni, *J. Phys.: Condens. Matter* **17**, S3709 (2005); M. Borromeo

- and F. Marchesoni, *Phys. Rev. E* **73**, 016142 (2006) .
- [4] H. J. Breymayer, *Appl. Phys. A* **33**, 1 (1984).
- [5] Goychuk, I., Hänggi, P., *Europhys. Lett.* **43**, 503 (1998).
- [6] M. Schiavoni, L. Sanchez-Palencia, F. Renzoni, and G. Grynberg, *Phys. Rev. Lett.* **90**, 094101 (2003); R. Gommers, S. Bergamini, F. Renzoni, *Phys. Rev. Lett.* **95**, 073003 (2005); F. Renzoni, *Cont. Phys.* **46**, 161 (2005).
- [7] M. Brown and F. Renzoni, *Phys. Rev. A* **77**, 033405 (2008) .

- [8] S. Flach, O. Yevtushenko, and Y. Zolotaryuk, Phys. Rev. Lett. **84**, 2358 (2000); S. Denisov, S. Flach and P. Hänggi, in: *Nonlinearities in Periodic Structures and Metamaterials*, C. Denz, S. Flach, and Y. Kivshar, eds. Springer Series in Optical Sciences vol. 150 (2010) 181 Springer.
- [9] R. Monaco, J. Appl. Phys. **68**, 679 (1990).
- [10] P. Hänggi, R. Bartussek, P. Talkner, and J. Luczka, Europhys. Lett. **35**, 315 (1996).
- [11] R. Kubo, Rep. Prog. Phys. **29**, 255 (1966).
- [12] W.C. Stewart, Appl. Phys. Lett. **12**, 277(1968); D. E. McCumber, J. Appl. Phys. **39**, 3113 (1968); R. L. Kautz, Rep. Prog. Phys. **59**, 935 (1996).
- [13] A. Barone and G. Paternò, *Physics and Application of the Josephson Effect*, Wiley, New York, (1982).
- [14] P. Hänggi and P. Jung, Adv. Chem. Phys. **89**, 239 (1995).
- [15] J. Luczka, Chaos **15**, 026107 (2005).
- [16] I. Goychuk and P. Hänggi, Adv. Phys. **54**, 525 (2005).
- [17] R. Zwanzig, J. Stat. Phys. **9**, 215 (1973).
- [18] P. Hänggi, Lect. Notes Phys. **484**, 15 (1997).
- [19] G.E. Uhlenbeck and L.S. Ornstein, Phys. Rev. **36**, 823 (1930).
- [20] L. Schimansky-Geier, C. Züllicke, Z. Phys. B **79**, 451 (1990).
- [21] T. Srokowski and M. Poszajczak, Phys. Rev. E **57**, 3829 (1998)
- [22] I. Goychuk, Phys. Rev. E **80**, 046125 (2009)
- [23] R. Kupferman, J. Stat. Phys. **114**, 291 (2004).
- [24] J. -D. Bao, Phys. Rev. E **69**, 016124 (2004).
- [25] J. Luczka, Physica A **153**, 619 (1988).
- [26] M. Kostur, J. Luczka, and P. Hänggi, Phys. Rev. E **80**, 051121 (2009).
- [27] L. Machura, M. Kostur and J. Luczka, Biosystems **94**, 253 (2008).
- [28] R. L. Honeycutt, Phys. Rev. A **45** 600 (1992).
- [29] M. Januszewski and M. Kostur, Comput. Phys. Commun. **181** 183 (2010).
- [30] E. Neumann and A. Pikovsky, Eur. Phys. J. B **26**, 219 (2002); R. Chacón and N. R. Quintero, BioSystems **88**, 308 (2007).
- [31] N. R. Quintero, J. A. Cuesta, and R. Alvarez-Nodarse, Phys. Rev. E **81**, 030102 R (2010).
- [32] R. Gommers, S. Bergamini, and F. Renzoni, Phys. Rev. Lett. **95**, 073003 (2005); A. B. Kolton and F. Renzoni, Phys. Rev. A **81**, 013416 (2010) and refs therein.
- [33] L. Machura, M. Kostur and J. Luczka, Chem. Phys. (2010), doi: 10.1016/j.chemphys.2010.03.008.
- [34] O. Yevtushenko, S. Flach, Y. Zolotaryuk and A. A. Ovchinnikov, Europhys. Lett. **54** (2001) 141.
- [35] S. Denisov and S. Flach, Phys. Rev. E **64**, 056236 (2001).
- [36] <http://fizyka.us.edu.pl/biharmonic>